This article has been accepted for publication in a future issue of this journal, but has not been fully edited. Content may change prior to final publication. Citation information: DOI 10.1109/TIA.2018.2853133, IEEE Transactions on Industry Applications

Impact of Punching Parameter Variations on Magnetic Properties of Non-Grain Oriented Electrical Steel

Hannes A. Weiss, Philipp Tröber, Roland Golle, Wolfram Volk
Technical University of Munich
Chair of Metal Forming and Casting
Walther-Meissner-Strasse 4
85748, Garching, Germany
Hannes.Weiss@utg.de

Simon Steentjes, Nora Leuning, Silas Elfgen, Kay Hameyer, Senior Member, IEEE
RWTH Aachen University
Institute of Electrical Machines
Schinkelstrasse 4
52062, Aachen, Germany

***Abstract*—The efficiency and performance of an electrical machine depends on the magnetic properties of its magnetic core, i. e., the rotor and stator core made of stacked and processed electrical steel laminations. Especially mechanical cutting, also known as punching or blanking, deteriorates the magnetic material properties next to the cutting line due to induced residual stress. The extent of the deterioration depends on the amount of induced stress, which is affected by the mechanical material properties and the process parameters used during punching. For this reason, in this paper the effect of punching parameter variations on the magnetic properties of eight different non-grain oriented electrical steels is investigated by using a single sheet tester. The magnetic property deterioration is discussed based on the specific-loss and the maximum field strength increase. In addition, the impact of punching parameter variations on the efficiency and the local flux and loss distribution of a permanent magnet synchronous machine is shown based on a finite element analysis. This allows one to tailor the punching parameters towards energy-loss minimization.**

***Index Terms*—blanking, cutting, magnetomechanical effects, magnetic losses, magnetic hysteresis, permanent magnet machine, punching, soft magnetic materials.**

I. Introduction

Rotor and stator cores of electrical machines are built up from stacked non-oriented electrical steel laminations. The overall efficiency and performance of an electrical machine strongly depends on alloying elements, thickness and heat treatment of the material used. Besides these influencing factors, the production process significantly alters the magnetic properties of rotor and stator cores, which results in a decreased machine efficiency and power density [1], [2]. This behavior is caused by the inverse magnetostrictive effect, which describes the change of a material's magnetizability depending on the induced mechanical stress [3]. Whether if it is the cutting, stacking or assembly process when building up a rotor or stator of an electrical machine, mechanical stress is induced in each manufacturing step. Next to the negative effect when interlocking or welding a rotor or stator stack, the cutting process significantly alters the magnetic properties of electrical steel sheets [4–7]. In order to measure the influence cutting has on the magnetic properties, standardized characterization methods like Epstein, single sheet or toroidal ring tests are modified. By separating the analyzed electrical steel strips, sheets or rings into smaller pieces, cutting related magnetic property deteriorations can be investigated [8, 9]. Reference [10] shows the negative influence of different cutting techniques like guillotining, punching and laser cutting on the magnetic material properties. In comparison to guillotining and punching, where plastic and elastic deformations lead to residual stress next to the cutting surface, laser cutting leads to thermal stress because of heating and cooling of the material [11]. Cutting electrical steel by waterjet or spark erosion minimizes the area affected by the inverse magnetostrictive effect [12], [13].

Fig. 1 shows a brief comparison on how different cutting

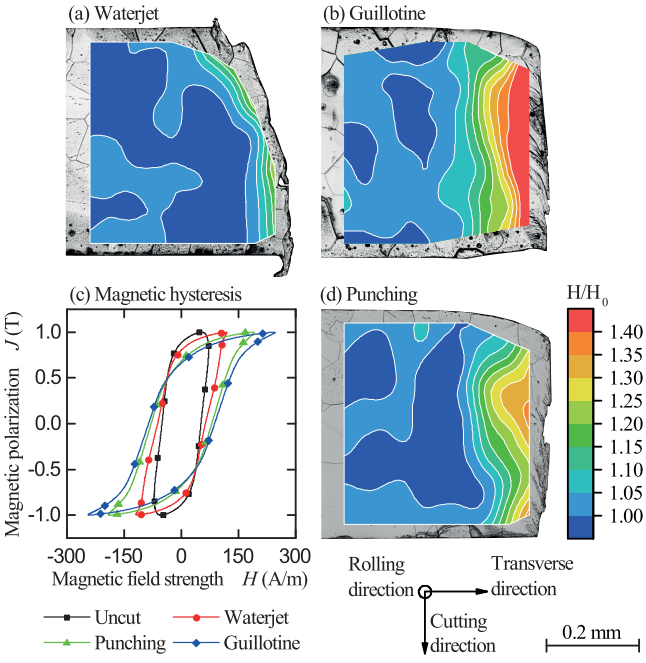

Fig. 1 Influence of the three different cutting techniques waterjet cutting (a), guillotining (b) and punching (d) on material hardness next to the cutting surface as well as on the magnetization behavior at 100 Hz and 1.0 T in rolling direction (c) [20]

This article has been accepted for publication in a future issue of this journal, but has not been fully edited. Content may change prior to final publication. Citation information: DOI 10.1109/TIA.2018.2853133, IEEE Transactions on Industry Applications

techniques affect the resulting cutting surface, material hardness and magnetic material properties. The electrical steel grade M270-50A has been processed by waterjet cutting, punching and guillotining. The magnetic analysis is carried out using a single-sheet–tester (SST) according to [14]. Fig. 1 displays local material hardness H with respect to virgin material hardness H_0 as well as differences in magnetic behavior at 100 Hz and 1.0 T. The cutting line and magnetic field orientation are aligned in rolling direction. A correlation between process-related material hardening and magnetic property degradation can be noticed. In comparison to waterjet cutting, punching and guillotining lead to increased material hardening due to plastic material deformation. Thereby, more residual stress is induced into the area next to the cutting surface. This results in increased hysteresis shearing, which leads to higher magnetic field strengths being needed to reach the same magnetic polarization. In addition, specific losses rise with increasing material deformation. Although punching and guillotining both belong to the mechanical cutting techniques, the resulting cutting surface, the material hardening and their effect on the magnetic properties differ. One reason for this behavior can be found in the rather soft machine setup of a guillotine compared with a stiff stamping-tool-mechanical-stamping-press-setup when punching.

Taking a closer look on the punching process, it can be noticed that even small changes like alternating punching parameters result in different residual stress states [15]. Using worn instead of sharp cutting edges for example leads to larger plastic material deformations and thereby more residual stress [15]. Residual stress impact on the magnetic behavior also depends on magnetic field strength and frequency [16]. Additionally, the induced residual stress magnitude as well as the proportion of tensile and compressive stress affects the magnetizability of an electrical steel [17–19].

The influence of a punching-related magnetic property deterioration when processing different electrical steel grades has not been investigated in detail until now. By comparing the impact of punching parameter variations on the magnetizability of eight different alloyed, rolled and heat-treated electrical steels, an optimized manufacturing strategy that leads to minimized specific losses can be found. The punching parameters investigated include changing cutting clearance and punching tools with different cutting edge wear states. This analysis allows a better consideration of punching related losses when designing new electromagnetic components. In addition, the results are transferable to other non-grain oriented electrical steel grades. In order for this goal to be achieved, a combined mechanical and magnetic investigation of punched electrical steels is required.

Parts of this work have been already presented at the International Electric Machines and Drives Conference (IEMDC) 2017 [20]. In addition to the conference version, the introduction has been extended, next to the specific-loss-factor the field-strength-factor is calculated, the impact of punching on the shape of the magnetic hysteresis and a numerical analysis of the deteriorated operating behavior of a permanent magnet synchronous machine (PMSM) due to punching parameter variations is added within this paper.

II. MATERIALS

For this investigation, eight different electrical steel grades are analyzed. The materials have been chosen in such a way that a wide field of application can benefit from the results. Processing influence is examined for four different sheet thicknesses s_0 0.3, 0.35, 0.5 and 0.65 mm. The materials have a silicon content ranging between 1.5 and 2.8 wt % and have been rolled and heat-treated differently. This results in a broad spectrum of different effective grain sizes, material hardnesses as well as mechanical and magnetic properties. All investigated materials are coated with an inorganic C-5 coating with organic components. [20]

All electrical steels used are metallographically, mechanically, chemically and magnetically characterized. Average grain size d_g is determined analyzing micrographs according to EN ISO 643. A micro hardness tester is used to measure virgin material hardness according to Vickers. Mechanical characteristics like ultimate tensile strength R_m or uniform elongation A_g are determined in tensile tests according to EN ISO 6892-1. In addition, magnetic properties are

TABLE I
THICKNESS, SILICON CONTENT, MECHANICAL AND MAGNETIC PROPERTIES OF THE INVESTIGATED MATERIALS [20]

Material	Thickness s_0 (µm)	Average grain size d_g (µm)	Si (wt %)	Material hardness (HV02)	Mechanical properties		Specific loss P_s (W/kg)		Magnetic polarization J (T)	
					R_m (MPa)	A_g (%)	1.0 T 50 Hz	1.5 T 50 Hz	2,500 A/m 50 Hz	5,000 A/m 50 Hz
A	300	107	2.8	226	596	8.4	1.08	2.60	1.53	1.62
B	350	87	2.8	227	613	9.1	1.30	2.93	1.55	1.63
C	350	70	2.4	196	527	11.0	1.42	3.31	1.55	1.63
D	350	58	1.5	168	429	14.7	1.63	3.46	1.67	1.75
E	500	111	2.8	224	578	8.4	1.26	2.92	1.55	1.63
F	650	121	2.8	221	589	9.3	1.64	3.65	1.57	1.65
G	650	102	2.4	195	513	11.1	1.78	4.08	1.58	1.66
H	650	98	1.5	171	407	14.4	1.99	4.44	1.66	1.74

This article has been accepted for publication in a future issue of this journal, but has not been fully edited. Content may change prior to final publication. Citation information: DOI 10.1109/TIA.2018.2853133, IEEE Transactions on Industry Applications

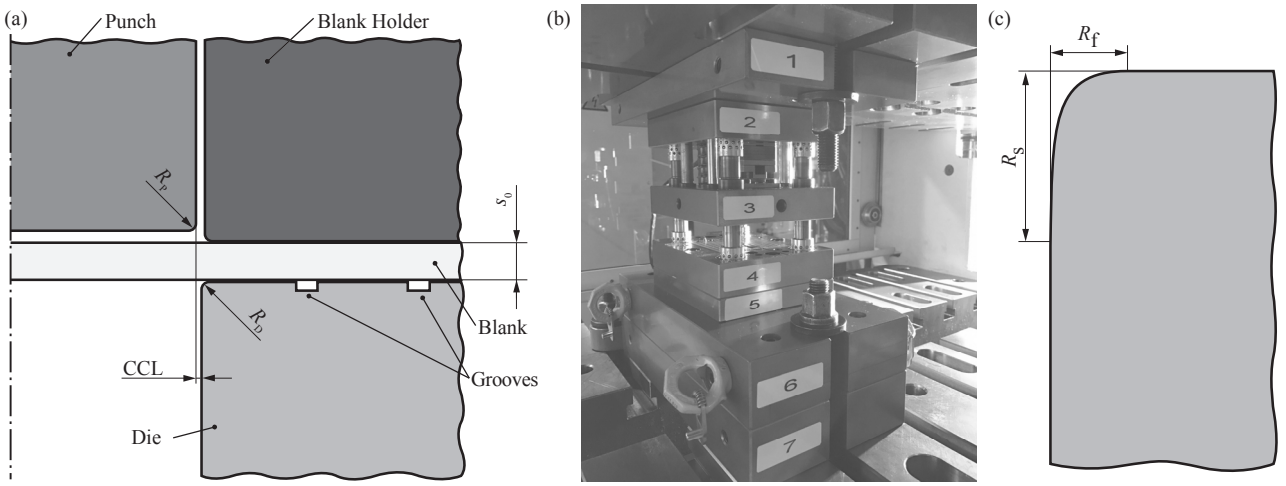

Fig. 2 (a), Punching tool sketch; (b), Punching tool inside the mechanical stamping press; (c), Cutting edge chamfer [20]

TABLE II
INVESTIGATED CCL AND CCL-SHEET-THICKNESS-RATIO [20]

s_0 (µm)	CCL (µm)				
	15	19	35	50	70
	CCL/s_0 (%)				
300	5.0	-	11.7	-	-
350	-	5.4	10.0	-	-
500	-	-	7.0	10.0	-
650	-	-	5.4	-	10.8

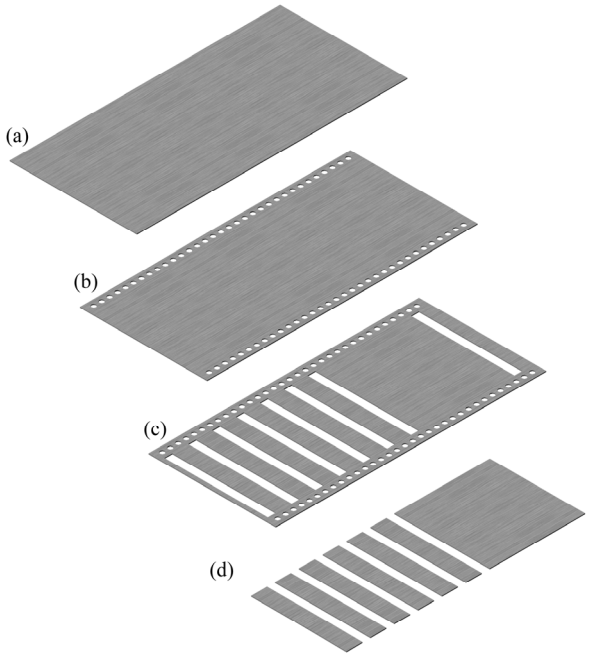

Fig. 3 Manufacturing process of single sheet tester specimens; (a), uncut sheet; (b), punching the positioning grid; (c), punching of six 10 mm specimen and one 60 mm specimen with various different process parameters; (d), positioning grid removal [20]

determined by using a 60 x 60 mm SST according to EN 10106. Table I shows the material properties investigated. Mechanical and magnetic properties displayed are average values of measurements in rolling direction (RD) and transverse direction (TD).

Due to the different alloys, cold rolling and heat treatment strategies the ratio of sheet thickness to average grain size reaches from 2.8 for material A to 6.6 for material H. High silicon contents lead to larger average grain size, elevated material hardness, higher ultimate tensile strengths and lower uniform elongation. The specific loss P_s also decreases with increasing silicon content at constant sheet thicknesses.

III. EXPERIMENTAL SETUP

A. Specimen punching

A high-precision punching tool in four-pillar design enables the production of specimen for electromagnetic investigations by using specific cutting parameters. The tool is operated with a mechanical stamping press at 100 strokes per minute. Punches and dies are made of a tungsten carbide tool material that is also used in industrial processing of electrical steel. A sketch of the basic tool construction and the real punching tool setup is shown in Fig. 2 (a) and Fig. 2 (b).

During the actual punching process, the sheet metal is clamped between blank holder and die. The material is then cut by the punch that travels towards the die. Grooves milled into the die help prevailing burr at the generated cutting surfaces from getting deformed when cutting small sample widths and therefore changing the process-related residual stress state. An integrated piezo force and inductive tool travel measurement system allow an online punching process monitoring with 100.000 samples per second.

Cutting clearance (CCL) and wear state of punch R_P and die R_D have a great effect on the induced residual stress when punching electrical steel [15]. In order to investigate the impact of process-related residual stress on magnetic property degradation, punch and die can be changed. This allows to realize CCLs from 15 to 70 µm. The dimensions are selected in

This article has been accepted for publication in a future issue of this journal, but has not been fully edited. Content may change prior to final publication. Citation information: DOI 10.1109/TIA.2018.2853133, IEEE Transactions on Industry Applications

such a way that similar CCL-sheet-thickness-ratios can be examined for different materials. Table II gives an overview of CCL used. Since the impact of tool wear is also investigated, an additional punch and die with grinded cutting edges at a CCL of 35 µm exist. The cutting edge chamfer geometry, a tangent-continuous ellipse with the two dimensions R_f and R_s, is shown in Fig. 2 (c). The machined edges represent a carbide tool wear after punching a 0.3 mm electrical steel for four million times ($R_{f,4mil}$ = 70 µm, $R_{s,4mil}$ = 100 µm). The worn cutting edges are referred to as 'worn' and new cutting edges ($R_{f,0}$ = 5 µm, $R_{s,0}$ = 5 µm) without any wear as 'sharp'.

The specimen manufacturing process for electromagnetic determination of the punching influence is shown in Fig. 3. Sheet metal strips with a dimension of 165 x 82.5 mm are cut parallel and transverse to RD from the electrical sheets (Fig. 3 (a)). This permits an examination of the punching influence as a function of cutting line position relative to rolling direction. Afterwards, a positioning grid, which guarantees a constant specimen width, is punched into the sheet metal strips (Fig. 3 (b)). Subsequently, the strips are punched with specific process parameters. Depending on the positioning of the rectangular cutout, strip widths of 5 to 60 mm can be produced as shown in Fig. 3 (c). Finally, the positioning grid is removed so that sheet metal strips with a variable width and a length of 60 mm are created. Fig. 3 (d) shows a 60 x 60 mm and six 10 x 60 mm samples.

B. Characterizing punching-related losses

Measuring the degraded electromagnetic properties of punched electrical steel is made possible by inserting more residual-stress-affected material volume into the measuring volume of a 60 mm x 60 mm single sheet tester. The electromagnetic properties are tested at excitation frequencies f of 10, 50, 100 and 400 Hz. Maximum magnetic polarizations J_{max} of 0.5, 1.0, 1.5 and 1.8 T are investigated. Magnetization direction is always aligned within the same direction as the cutting line. The SST is integrated into a computer-assisted test set-up according to international standard IEC 60404 3.

When determining the punching-related electromagnetic property degradation, first an electrical steel specimen with dimensions of 60 x 60 mm is examined. As a result of increasing cutting line length due to reduction of sheet metal strip width at constant material volume, more and more stress affected material is inserted into the single sheet testers' measuring volume. When twelve 5 x 60 mm strips are tested, the cutting line length as well as residual stress affected material volume increases by a factor of twelve compared to a 60 x 60 mm specimen. A comparison of measurements with varying cutting line length at different magnetic field intensities and excitation frequencies allows a detailed investigation of punching process parameter variations.

IV. Results

First the magnetic property degradation due to punching is examined depending on the cutting line orientation to RD.

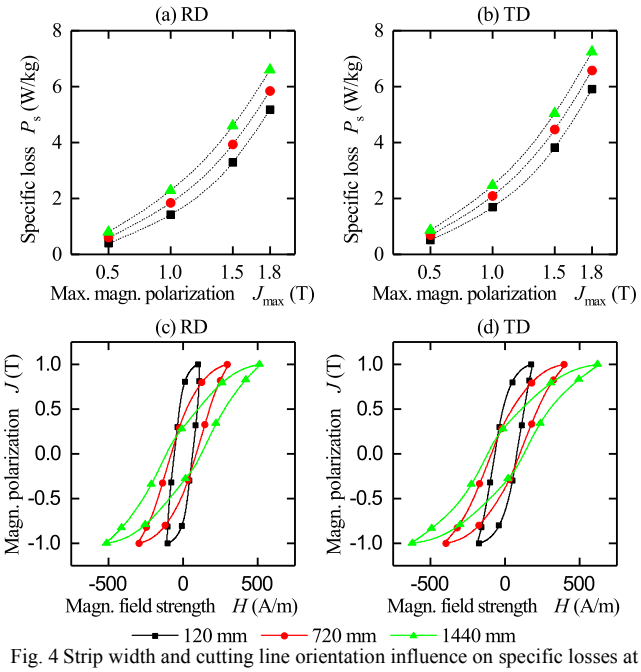

Fig. 4 Strip width and cutting line orientation influence on specific losses at varying polarizations (a, b) as well as on the hysteresis curve (c, d) of material F at 50 Hz [20]

Therefore, cutting line lengths of 120, 720 and 1440 mm, which correspond to the specimen quantity and size of one 60 x 60 mm, six 10 x 60 mm and twelve 5 x 60 mm are investigated. Fig. 4 shows specific losses (a, b) and magnetic hysteresis (c, d) measured at 50 Hz and at different maximum magnetic polarizations for material F depending on the orientation of the cutting line to RD. Specimens were punched using a CCL of 10.8 % and sharp cutting edges.

Higher specific losses can be noticed for an increasing cutting line length, independent of the specimen orientation. The maximum magnetic field strength needed to reach the same polarization levels also increases. Looking at different orientations to rolling direction, specific losses and hysteresis shearing are slightly elevated when the cutting line is oriented in rolling direction.

Calculating an orientation dependent specific-loss-factor $C_{s,OR}$ with specific losses $P_{s,1440,OR}$ at 1440 mm and $P_{s,120,OR}$ at 120 mm cutting line length according to (1) helps analyzing the magnetic property degradations.

$$C_{s,OR}(J_{max}, f) = \frac{P_{s,1440,OR}(J_{max}, f)}{P_{s,120,OR}(J_{max}, f)} \quad (1)$$

In case of a cutting line orientation variation, the specific-loss-factor changes from 1.46 in TD to 1.62 in RD at a magnetic polarization of 1.0 T and an excitation frequency of 50 Hz. At elevated magnetic polarizations of 1.8 T the specific-loss-factor varies from 1.23 in TD to 1.28 in RD. A higher impact on magnetic property degradation when punching in RD can be observed regardless of the material examined. In order to simplify the result analysis, an orientation independent specific-loss-factor C_s can be calculated according to (2).

This article has been accepted for publication in a future issue of this journal, but has not been fully edited. Content may change prior to final publication. Citation information: DOI 10.1109/TIA.2018.2853133, IEEE Transactions on Industry Applications

$$C_{\mathrm{s}}(J_{\max}, f) = \frac{C_{\mathrm{s,RD}}(J_{\max}, f) + C_{\mathrm{s,TD}}(J_{\max}, f)}{2} \quad (2)$$

In Fig. 5 the influence of residual stress due to punching with 11.7 % CCL for material A, 10.0 % CCL for material B, C, D, E, 10.8 % CCL for material F, G, H and sharp cutting edges at different excitation frequencies and varying maximum magnetic polarizations is shown. The specific-loss-factor due to punching significantly depends on the magnetic polarization and excitation frequency. Major punching impacts can be observed at low frequencies and low polarization levels. The specific-loss-factor can reach up above 2.05 for electrical steel grade F at 0.5 T and 10 Hz. Even at polarizations of 1.8 T at 100 Hz the specific-loss-factors still reaches 1.19. Looking at different electrical steel grades, the specific-loss-factor rises with a growth in sheet thickness. Additionally, materials with high silicon content and high ultimate tensile strength are more affected by punching induced residual stress.

The impact of a punching parameter variation on the first hysteresis quadrant of material C is shown in Fig. 6 for different maximum magnetic polarizations at an excitation frequency of 50 Hz and a cutting line orientation in TD. Small CCL and a sharp cutting edge lead to less induced stress and, therefore, less hysteresis shearing. This is particularly noticeable at polarizations up to the knee of the magnetic hysteresis, where the magnetization process is dominated by domain wall movement. Here, stress and dislocations induced by banking deteriorate the magnetic properties to a big extent.

The punching-related loss increases for different maximum magnetic polarizations at an excitation frequency of 50 Hz are depicted in Fig. 7 for each material investigated. In addition, Fig. 8 shows the extent of punching parameter variations on the maximum magnetic field strength needed to reach the desired polarization. Therefore, a field-strength-factor C_{Hmax} is calculated similar to the specific-loss-factor in (1) and (2). The punching parameter variations discussed, range from 5.0 % to 11.7 % CCL and from a sharp to a worn cutting tool edges.

Regardless of the electrical steel grade observed, the possibility to reduce the specific-loss-factor using optimized punching parameters gets smaller when operating electrical steels at rising maximum magnetic polarization levels. This

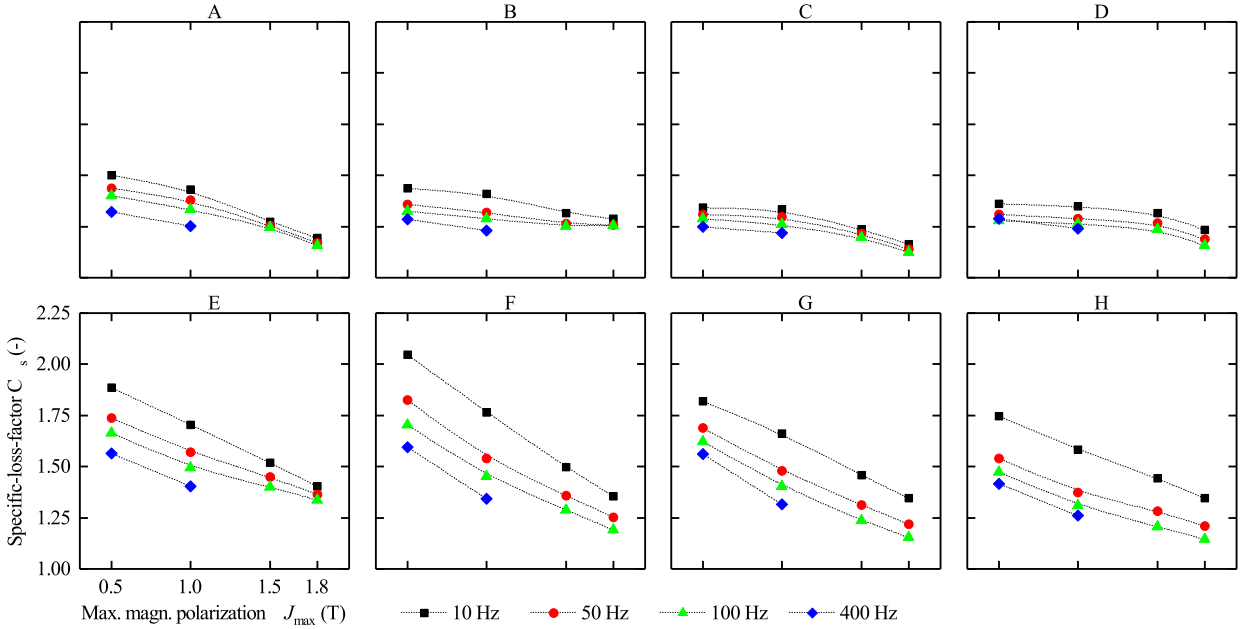

Fig. 5 Specific loss increase when punching with 11.7 % CCL for material A, 10.0 % CCL for material B, C, D, E, 10.8 % CCL for material F, G, H and sharp cutting edges at different excitation frequencies and varying maximum magnetic polarizations [20]

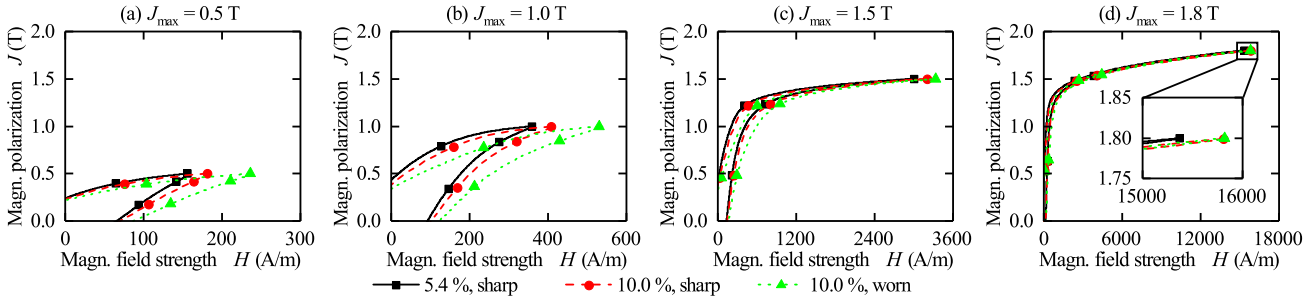

Fig. 6 Impact of punching in TD with different parameters on the magnetic hysteresis of material C at varying maximum polarization levels and at 50 Hz

This article has been accepted for publication in a future issue of this journal, but has not been fully edited. Content may change prior to final publication. Citation information: DOI 10.1109/TIA.2018.2853133, IEEE Transactions on Industry Applications

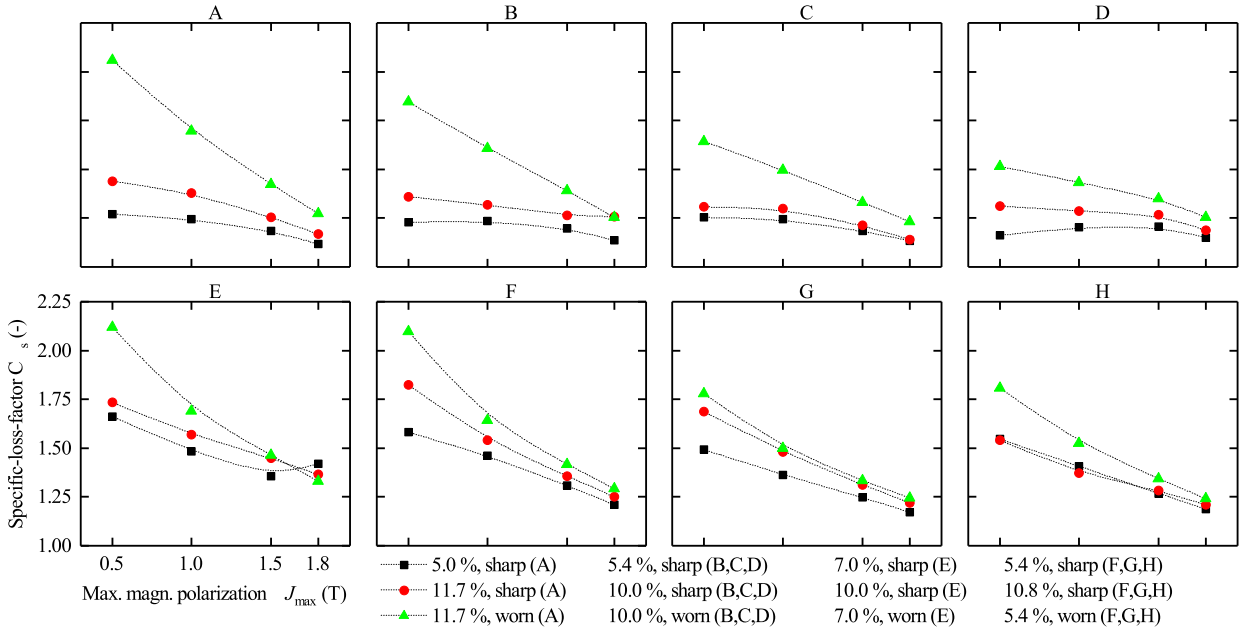

Fig. 7 Punching parameter influence on specific-loss-factor for material A to H at an excitation frequency of 50 Hz and at varying magnetic polarizations [20]

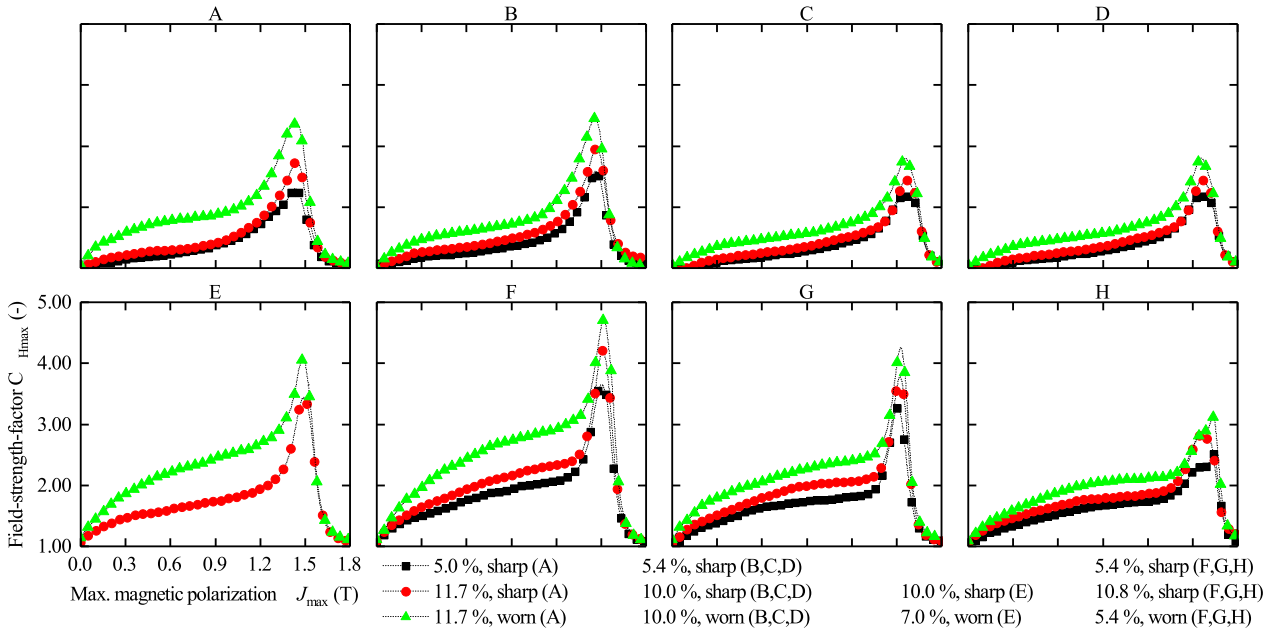

Fig. 8 Punching parameter influence on field-strength-factor for material A to H at an excitation frequency of 50 Hz and at varying magnetic polarizations

behavior can also be examined at elevated excitation frequencies. Apart from that, the possibility of reducing specific loss by using optimized punching parameters can improve performance of electrical machines that are operated at low polarization and frequency levels is still given.

Comparing different punching parameter variations to each other, it can be noticed that higher CCL as well as worn cutting edges result in higher specific-loss-factors and higher field-strength-factors. Punching with small cutting CCL and sharp cutting edges leads to minimized specific loss and maximum magnetic field strength increases. Overall cutting edge wear has a larger impact on specific loss and maximum magnetic field strength increase than the effect of a CCL variation.

Taking different electrical steel grades into account, it can be recognized that materials with high ultimate tensile strength (A, B, E, and F) can be influenced to a larger extent than materials with lower ultimate tensile strength (C, D, G, and H). Especially cutting edge wear state has a bigger impact on magnetic property deterioration when looking at electrical steel grades with higher ultimate tensile strength. Similar to the specific-loss-factor the materials ultimate tensile strength also has a large impact on the field-strength-factor with high

This article has been accepted for publication in a future issue of this journal, but has not been fully edited. Content may change prior to final publication. Citation information: DOI 10.1109/TIA.2018.2853133, IEEE Transactions on Industry Applications

strength materials showing a larger influence. Comparing the field-strength-factor for materials with the same silicon content (A, B, E, F – C, G – D, H) to each other a larger impact can be noticed when punching thicker electrical steel laminations.

As already mentioned, the deterioration of the magnetic properties is directly related to the punching induced stress. It results from the material deformation taking place during the separation process. The punch force over punch travel curve indicates the quantity of deformed material volume [21]. Analyzing it can help reducing the amount of magnetic property degradation, even in the industrial manufacturing process of rotor and stator cores. In order to demonstrate this correlation, punch force over punch travel curves for the electrical steel grades F and H cut with sharp and worn tools are shown in Fig. 9. Both graphs indicate that the punching work, the area under the punch force over punch travel curve, is increased when cutting with a worn tool. Since, the work needed for the separation process is related to the amount of deformed material, more stress is induced when punching with a worn tool. This interdependence, that is also shown in [15], matches with the results of the specific-loss-factor and the field-strength-factor analysis discussed above. Therefore, measuring the punch force over punch travel curve can help limiting magnetic property deterioration because of an increasing amount of punching induced stress.

V. Simulation of Cutting Related Loss Increases

The impact of the punching related magnetic property deterioration on the flux density distribution and the specific loss distribution is numerically analyzed regarding the stator of a PMSM. The investigation helps understanding the extent punching has on the losses generated within an electrical machine. In addition, the benefit of taking punching related magnetic property deteriorations for a numerical simulation of an electrical machine into account is shown in this section.

The investigations are carried out for a virgin and two deteriorated magnetic material behaviors. The punching affected material behavior from the electrical steel C processed with 10 % CCL for sharp and worn cutting edges is examined in the finite element simulation. For the investigations the PMSM studied in [22] is used. A cross section of the machine geometry is shown in Fig. 10. The geometrical data as well as the machine characteristics at the nominal working point are presented in table III. In the simulation the local magnetic material mode presented in [23] is used to consider the magnetizability of the material with respect of the distance to the cutting surface.

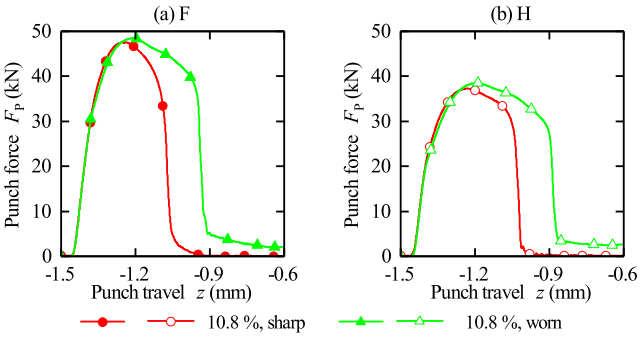

Fig. 9 Punch force over punch travel for material F and H processed with 10.8 % CCL using sharp and worn cutting edges [20]

The calculation of the resulting specific loss parameters are conducted from the SST measurement data. In order to identify the different loss contributions from measured data, the iron loss model presented in [24] is used. The specific loss model in (3) considers the contributions of static hysteresis P_{hyst}, eddy currents P_{cl}, excess P_{exc} and saturation losses P_{sat}.

$$P_{\mathrm{s}} = P_{\mathrm{hyst}} + P_{\mathrm{cl}} + P_{\mathrm{exc}} + P_{\mathrm{sat}} \tag{3}$$

The loss contributions are calculated according to (4)-(7).

$$P_{\mathrm{hyst}} = a_1 \left(1 + \frac{B_{\min}}{B_{\max}} \left(r_{\mathrm{hyst}} - 1 \right) \right) B_{\max}^{\alpha} f_1 \tag{4}$$

$$P_{\mathrm{cl}} = a_2 \sum_{n=1}^{\infty} \left(B_{\mathrm{n}}^2 \, (nf)^2 \right) \tag{5}$$

$$P_{\mathrm{exc}} = a_2 \sum_{n=1}^{\infty} \left(B_{\mathrm{n}}^{1.5} \, (nf)^{1.5} \right) \tag{6}$$

$$P_{\mathrm{sat}} = a_2 a_3 B_{\max}^{a_4+2} f_1^2 \tag{7}$$

In the classical iron loss calculation eddy current losses are calculated analytically as described in (5). This loss separation was found to be inaccurate especially for frequencies above 400Hz and high magnetic polarization values [24]. To cope with strongly increasing iron specific losses also due to the skin effect the additional term of the saturation losses is considered in the formulation of the iron losses.

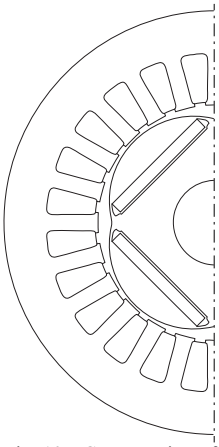

Fig. 10 Cross section of the machine geometry

TABLE III
Geometrical Data and Machine Characteristics of Nominal Working Point

Parameter	Symbol	Value
Stator outer diameter	$D_{\mathrm{s,o}}$	90 mm
Rotor outer diameter	$D_{\mathrm{r,o}}$	49 mm
Stator tooth width	$w_{\mathrm{S,t}}$	4.2 mm
Yoke width	$w_{\mathrm{S,y}}$	9 mm
Slots	N	24
Pole pairs	p	2
Speed	N_{n}	1,500 min^{-1}
Power	P_{n}	219 W
Torque	M_{n}	1.44 N m
Efficiency	η_{n}	82.50 %
Iron losses	$P_{\mathrm{s,n}}$	5 W
Copper losses	P_{cu}	40 W

This article has been accepted for publication in a future issue of this journal, but has not been fully edited. Content may change prior to final publication. Citation information: DOI 10.1109/TIA.2018.2853133, IEEE Transactions on Industry Applications

The iron loss components calculated with the different magnetic materials states are listed in table IV. Except for the classical eddy losses P_{cl} and the saturation losses P_{sat} each loss component rises when the material is more damaged and more residual stress is induced. The smaller classical eddy current losses and saturation losses can be explained with the smaller amount of material volume that is able to be magnetized due to the large amount of induced stress and dislocations near the cutting surface.

In Fig. 11 the resulting local flux density and specific loss distribution is depicted on the machine geometry. In (a) and (d), an unaffected material property is depicted, while a local permeability distribution is considered in (b) and (e) as well as in (c) and (f). In (b) and (e) the magnetic property of material C punched with 10 % CCL and sharp cutting edges is used. In (c) and (f) the magnetic property of material C punched with 10 % CCL and worn cutting edges is used. Already from undamaged (a) to the cut edge affected material property (b) or (c), a concentration of the flux density to the center of the yoke and the tooth can be seen. This is due to the reduced permeability along the cutting lines. Comparing both damaged models (b) and (c) with each other, a further reduction of the flux at the edges of the tooth and the yoke result in case of (c).

While for high induction levels of e.g. 1.8 T the effect of flux concentration is less pronounced, the influence on the resulting losses is still important. In Fig. 11 (d), (e) and (f) the influence on the resulting specific losses are depicted on the stator of the machine. Especially in case of the 10 % CCL, worn magnetic material state, a concentration of the flux density to the center of the material is observed, which leads to higher local loss densities in the center of the stator tooth and yoke. The corresponding global loss value along with each loss contribution are depicted in table IV. Here the influence of punching on the specific iron losses can be seen.

The simulation of the PMSM demonstrates that it is important to consider punching related magnetic property deterioration. Taking a local magnetic material model into account, allows a realistic prediction of magnetic flux density and specific loss distribution within an electrical machine.

The results also verify the analysis of the magnetic material degradation using the specific-loss-factor and the field-strength-factor. Hence, the efficiency and performance of future electrical machines can be improved by punching with small CCL and sharpening the cutting tools more often. Since tools having small CCL are expensive, they should only be used in appropriate areas, like stator or rotor teeth.

VI. Conclusion and Outlook

For the first time, these investigations allowed an analyzation of how punching processes affect magnetic material properties. Cutting clearance and cutting edge wear state variations were examined. A wide range of different electrical steel grades ensured that interactions between metallographic, mechanical and electromagnetic properties and punching process were identified. The results presented in this paper are intended to facilitate future electric drive layout and design and thus contribute to increasing energy efficiency as well as reducing carbon dioxide emissions.

TABLE IV
Iron loss components for the different states of material C

Material state	Undamaged	10 %, sharp	10 %, worn
Specific loss P_s (W)	2.96	4.25	4.95
Hysteresis loss P_{hyst} (W)	2.08	2.54	2.74
Classical loss P_{cl} (W)	0.11	0.10	0.06
Excess loss P_{ex} (W)	0.48	1.40	1.98
Saturation loss P_{sat} (W)	0.28	0.23	0.16

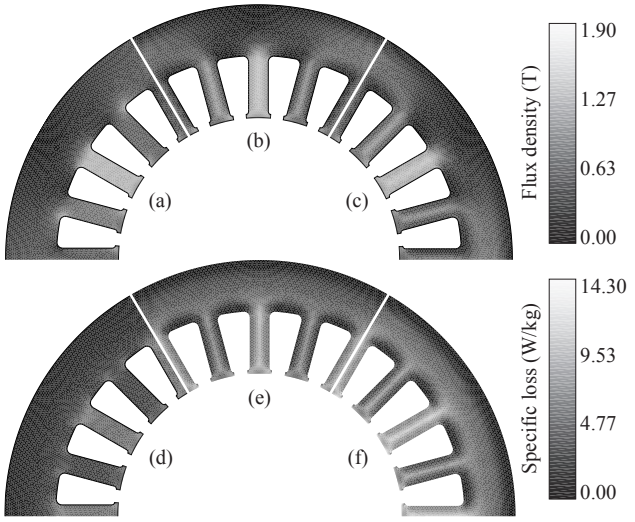

Fig. 11 Local magnetic flux and specific loss density considering (a, d), an undamaged magnetic material without local magnetic material model, (b, e), 10 % CCL, sharp material state and a local magnetic material model and (c, f), 10 % CCL, worn material state and a local magnetic material model

Regarding magnetic property degradation due to punching-related residual stresses, following effects have been observed:

- Increasing cutting line length and thereby rising stress affected volume inside the analyzed measurement volume leads to higher specific loss and larger hysteresis shearing. Varying mechanical and magnetic properties in rolling and transverse direction cause this behavior to differ depending on cutting line orientation.
- Specific loss increase due to residual stress reaches its maximum for low excitation frequencies and polarizations regardless of the investigated punching parameter set.
- Maximum magnetic field strength increase due to punching reaches a maximum at the knee of the magnetic hysteresis.
- A reduction of specific losses and maximum magnetic field strengths with optimized punching parameters is possible. The extent of specific losses that can be reduced depends on the excitation frequency and on the magnetic polarization. For example, specific loss increase has been reduced by up

to 80 % at frequencies of 50 Hz and polarizations of 0.5 T for electrical steel grade A.

- Punching-related magnetic property degradation strongly depends on the mechanical properties of an electrical steel grade. High ultimate tensile strength leads to an increased punching parameter sensitivity. For example, cutting edge wear state has far more influence on high strength electrical steel grades. Especially, when looking at the recent trend of using thin, high strength steel in electrical traction drives, punching can have a significant impact regarding their efficiency and performance.
- Less cutting clearance and less cutting edge wear can reduce specific loss as well as maximum magnetic field strength. An optimized cutting clearance has to be defined in the magnetic machine design process before ordering a new stamping tool. Cutting edge wear can be reduce by using a wear resistant punch and die material like tungsten carbide. Additionally, cutting edges have to be sharpened more often to reduce excessive plastic material deformations.

To improve electric machine simulations, not only the specific loss increases but also the penetration depth of residual stress affected material volume next to the cutting line needs to be known. First punching process finite element analysis in [15] show that the affected volume reaches 1 mm deep into the material outgoing from the cutting line. To validate these simulations, a neutron grating interferometry analysis of punched specimens will be presented in the near future. This analysis will help understanding up to which extent domain wall mobility is inhibited by local residual stresses at varying magnetic polarization levels.

ACKNOWLEDGMENT

This work is funded by the Deutsche Forschungsgemeinschaft (DFG, German Research Foundation) – 218259799, 255713208 and carried out in the research group project – "FOR 1897 – Low-Loss Electrical Steel for Energy-Efficient Electrical Drives".

REFERENCES

VII. REFERENCES

[1] A. Schoppa, J. Schneider, and C.-D. Wuppermann, "Influence of the manufacturing process on the magnetic properties of non-oriented electrical steels," *Journal of Magnetism and Magnetic Materials*, vol. 215-216, pp. 74–78, 2000.

[2] K. Yamazaki, H. Mukaiyama, and L. Daniel, "Effects of Multi-Axial Mechanical Stress on Loss Characteristics of Electrical Steel Sheets and Interior Permanent Magnet Machines," *IEEE Trans. Magn.*, pp. 1–4, 2017.

[3] R. M. Bozorth, "Ferromagnetism," 67–101, 595–712, 1978.

[4] S. Imamori, S. Steentjes, and K. Hameyer, "Influence of Interlocking on Magnetic Properties of Electrical Steel Laminations," *IEEE Trans. Magn.*, vol. 53, no. 11, pp. 1–4, 2017.

[5] K. Bourchas *et al.,* "Quantifying Effects of Cutting and Welding on Magnetic Properties of Electrical Steels," *IEEE Trans. on Ind. Applicat.*, vol. 53, no. 5, pp. 4269–4278, 2017.

[6] K. Fujisaki *et al.,* "Motor Core Iron Loss Analysis Evaluating Shrink Fitting and Stamping by Finite-Element Method," *IEEE Trans. Magn.*, vol. 43, no. 5, pp. 1950–1954, 2007.

[7] M. Bali and A. Muetze, "Influence of Different Cutting Techniques on the Magnetic Characteristics of Electrical Steels Determined by a Permeameter," *IEEE Trans. on Ind. Applicat.*, vol. 53, no. 2, pp. 971–981, 2017.

[8] K. H. Schmidt, "Influence of Punching on the Magnetic Properties of Electric Steel with 1% Silicon," *Journal of Magnetism and Magnetic Materials*, vol. 2, no. 1-3, pp. 136–150, 1975.

[9] A. Boglietti, "A first approach for the iron losses building factor determination," in *Conference Record of the 1999 IEEE Industry Applications Conference. Thirty-Forth IAS Annual Meeting (Cat. No.99CH36370)*, Phoenix, AZ, USA, Oct. 1999, pp. 489–493.

[10] M. Emura, F.J.G. Landgraf, W. Ross, and J.R. Barreta, "The influence of cutting technique on the magnetic properties of electrical steels," *Journal of Magnetism and Magnetic Materials*, vol. 254-255, pp. 358–360, 2003.

[11] R. Siebert, J. Schneider, and E. Beyer, "Laser Cutting and Mechanical Cutting of Electrical Steels and its Effect on the Magnetic Properties," *IEEE Trans. Magn.*, vol. 50, no. 4, pp. 1–4, 2014.

[12] A. Schoppa, H. Louis, F. Pude, and C. von Rad, "Influence of abrasive waterjet cutting on the magnetic properties of non-oriented electrical steels," *Journal of Magnetism and Magnetic Materials*, vol. 254-255, pp. 370–372, 2003.

[13] M. Hofmann, H. Naumoski, U. Herr, and H.-G. Herzog, "Magnetic Properties of Electrical Steel Sheets in Respect of Cutting: Micromagnetic Analysis and Macromagnetic Modeling," *IEEE Trans. Magn.*, vol. 52, no. 2, pp. 1–14, 2016.

[14] S. Steentjes *et al.,* "On the effect of material processing: microstructural and magnetic properties of electrical steel sheets," *IEEE Electric Drives Production Conference (EDPC), 4th International*, pp. 1–7, 2014.

[15] H. A. Weiss *et al.,* "Influence of shear cutting parameters on the electromagnetic properties of non-oriented electrical steel sheets," *Journal of Magnetism and Magnetic Materials*, vol. 421, pp. 250–259, 2017.

[16] N. Leuning, S. Steentjes, K. Hameyer, M. Schulte, and W. Bleck, "Effect of Material Processing and Imposed Mechanical Stress on the Magnetic, Mechanical, and Microstructural Properties of High-Silicon Electrical Steel," *steel research int.*, 2016.

[17] M. LoBue, C. Sasso, V. Basso, F. Fiorillo, and G. Bertotti, "Power losses and magnetization process in Fe–Si non-oriented steels under tensile and compressive stress," *Journal of Magnetism and Magnetic Materials*, vol. 215-216, pp. 124–126, 2000.

[18] N. Leuning, S. Steentjes, M. Schulte, W. Bleck, and K. Hameyer, "Effect of elastic and plastic tensile mechanical loading on the magnetic properties of NGO electrical steel," *Journal of Magnetism and Magnetic Materials*, vol. 417, pp. 42–48, 2016.

[19] H. Naumoski, A. Maucher, and U. Herr, "Investigation of the influence of global stresses and strains on the magnetic properties of electrical steels with varying alloying content and grain size," in *2015 5th International Electric Drives Production Conference (EDPC)*, Nuremberg, Germany, pp. 1–8.

[20] H. A. Weiss *et al.,* "Loss reduction due to blanking parameter optimization for different non-grain oriented electrical steel grades," in *2017 IEEE International Electric Machines and Drives Conference (IEMDC)*, Miami, FL, USA, pp. 1–7.

[21] T. Kopp *et al.,* "Experimental investigation of the lateral forces during shear cutting with an open cutting line," *Journal of Materials Processing Technology*, vol. 238, pp. 49–54, 2016.

[22] S. Elfgen, S. Steentjes, S. Bohmer, D. Franck, and K. Hameyer, "Influences of Material Degradation Due to Laser Cutting on the Operating Behavior of PMSM Using a Continuous Local Material Model," *IEEE Trans. on Ind. Applicat.*, vol. 53, no. 3, pp. 1978–1984, 2017.

[23] S. Elfgen, S. Steentjes, S. Bohmer, D. Franck, and K. Hameyer, "Continuous Local Material Model for Cut Edge Effects in Soft Magnetic Materials," *IEEE Trans. Magn.*, vol. 52, no. 5, pp. 1–4, 2016.

[24] S. Steentjes, M. Leßmann, and K. Hameyer, "Semi-physical parameter identification for an iron-loss formula allowing loss-separation," *Journal of Applied Physics*, vol. 113, no. 17, 17A319, 2013.